FROM STEP EDGE TO LINE EDGE: COMBINING GEOMETRIC AND PHOTOMETRIC INFORMATION

Alain Filbois and Didier Gemmerlé

CRIN/CNRS – INRIA Lorraine, Bâtiment LORIA,
Campus Scientifique, B.P. 239, 54506 Vandœuvre CEDEX France
EMAIL: ALAIN.FILBOIS@@LORIA.FR, DIDIER.GEMMERLE@@LORIA.FR

ABSTRACT

As a Gradient detector produces two extrema when applied to a line, we propose an original method which is based on such a detector but which appropriately res-ponds to both step and line edges. The main ideas are first to identify line contours using geometric and photometric properties and second to substitute a line for a single contour using a simple geometric algorithm.

1. INTRODUCTION

Early vision begins with the computation of a compact description of the raw image intensity. Physical edges provide fundamental visual information since they correspond to the discontinuities of the physical and photometrical properties of the objects. Consequently, edge detection consists in characterizing these variations in terms of the physical phenomena at their origin. The most common edge detectors deal with step edges [10, 2, 4]. However, a grey scale image contains various kinds of edges coming from different scene events and different physical phenomena. For example, an object on a uniform background or fingerprints give rise to line contours, called pulses or roofs, in the digitalized image. When applied to such an image, the Canny detector [2] or a similar one produces two extrema rather than one. For this reason, specific detectors, like line detectors [17] or ridge detectors [5, 7], have been created. Other line detectors directly work on binary or grey scale images using a thinning algorithm [12, 3]. However, a line or a ridge detector gives spurious responses to other kind of edges. Works have been proposed to select appropriate step edge detectors to find a given edge [8, 18]. Our approach focuses on both step and line edges.

We give in the second section the properties of the response of a line to a step edge detector. These properties are used to identify lines included in the image. The search and location of line edges include three steps. In the first step (cf. Section 3), all possible pairs of closed and parallel segments are considered as candidate lines. Pairs which are generated by lines must have the typical profiles of the roof and pulse edges. In the second step (cf. Section 4), the pairs of segments are connected to complete the corresponding line edge, and the extremities of the lines are examined. In the third step (cf. Section 5), the peaks are searched. Examples of the results we obtain are presented in sixth section.

2. PROPERTIES OF A LINE EDGE

We define the properties of a line edge in terms of the Gradient of the Gaussian in the following way (Fig. 1.a):

$$C(x) = A_0 H(x - l_0) - A_1 H(x - l_1),$$

where A_0 and A_1 are the left and right contrast of the line edge, and H is the Heavyside function [15]. The response

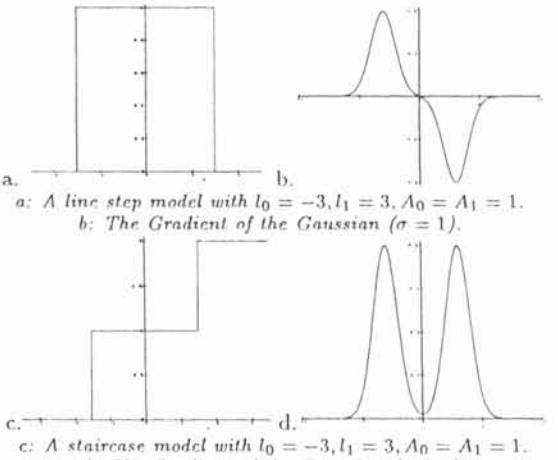

a: A line step model with $l_0 = -3, l_1 = 3, A_0 = A_1 = 1$.
b: The Gradient of the Gaussian ($\sigma = 1$).
c: A staircase model with $l_0 = -3, l_1 = 3, A_0 = A_1 = 1$.
d: The Gradient of the Gaussian ($\sigma = 1$).

Figure 1. The line step and staircase models *[Tab94]*.

of this model to the first derivative of the Gaussian is:

$$F_x(x, \sigma) = -\frac{1}{\sigma^2}(A_0 g_\sigma(x - l_0) - A_1 g_\sigma(x - l_1)),$$

where $g_\sigma(x) = \frac{1}{\sigma\sqrt{2\pi}} e^{-\frac{x^2}{2\sigma^2}}$ is the Gaussian filter. This response has two extrema (Fig. 1.b) which generate a double step in 2D. On these contours, an edge following [6] and a polygonal approximation [16, 9] generate two close segments, theoretically parallel, which are the edges of the line contour. However, a double contour can also be generated by a double step, shaped like a staircase (Fig. 1.c). With the same notations, a staircase model can be defined in the following manner [15]:

$$E(x) = A_0 H(x - l_0) + A_1 H(x - l_1),$$

$$F_x(x, \sigma) = -\frac{1}{\sigma^2}(A_0 g_\sigma(x - l_0) + A_1 g_\sigma(x - l_1)).$$

Figure 1.d shows the response of function F_x. The norm of the Gradient presents two extrema for both staircase and line models (fig. 1.b and 1.d).

We use the profile to characterize the two contour models. The profile of a double contour corresponds to the three means of the grey levels of the three zones respectively on the left hand side, in the middle and on the right hand side of the double contour. For a line edge model, the mean of the middle zone is either greater or less than the other two. For a staircase model, the mean of the middle zone is bounded by the other two. Therefore, a line is defined by its profile and two chains of parallel segments such as their distance is smaller than six times the standard deviation of the smoothing filter. This distance is roughly the size of the Gaussian filter [14, 15].

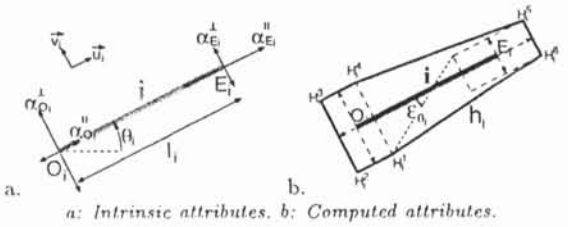

a: Intrinsic attributes. b: Computed attributes.

Figure 2. A segment and its attributes.

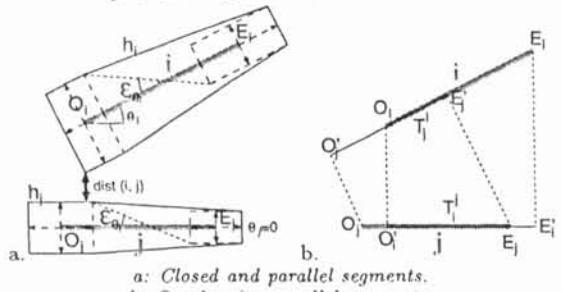

a: Closed and parallel segments.
b: Overlapping parallel segments.

Figure 3. Two segments i, j with (1), (2) and (3) fulfilled.

3. LINE STEP COMPUTATION

A segment i is characterized by intrinsic attributes: O_i, the origin of the segment, E_i, its extremity, l_i, its length and θ_i, the angle between the segment and the horizontal direction (Fig. 2.a). Each extremity S of i is associated with intrinsic attributes $\alpha^{\parallel}_S$ and $\alpha^{\perp}_S$ which represent the non-biased error on the location of S in directions respectively parallel and orthogonal to i. These attributes are assumed to be independent and define a so-called uncertainty rectangle for each extremity of i. A segment is considered as significative if $\alpha^{\parallel}_{O_i} + \alpha^{\parallel}_{E_i} \ll l_i$. Using these attributes, we define a so-called uncertainty hexagon h_i as the smallest region including i (Fig. 2.b). If $\alpha^{\perp}_{O_i} > \alpha^{\perp}_{E_i}$, the vertices $H_i^{1..6}$ of this hexagon are defined as follows:

$$\begin{cases} H_i^{1..4} = O_i \pm \alpha^{\parallel}_{O_i}.\vec{u_i} \pm \alpha^{\perp}_{O_i}.\vec{v_i} \\ H_i^{5..6} = E_i + \alpha^{\parallel}_{E_i}.\vec{u_i} \pm \alpha^{\perp}_{E_i}.\vec{v_i} \end{cases}$$

where $\vec{u_i}$ is the unit vector parallel to i and $\vec{v_i}$ is the unitary vector orthogonal to i. Each segment i is provided with a confidence rate which only depends on the error $\epsilon^{\theta}_i = \arctan(\frac{l_i - \alpha^{\parallel}_{O_i} - \alpha^{\parallel}_{E_i}}{\alpha^{\perp}_{O_i} + \alpha^{\perp}_{E_i}})$ on the attribute θ_i.

A pair C_{ij} of segments i and j are considered as parallel if:

$$| \theta_i - \theta_j | \leqslant \Upsilon + \epsilon^{\theta}_i + \epsilon^{\theta}_j \quad (1)$$

In our test data set, Υ varies from 1 to 4 degrees. The distance between two segments i and j is defined as $dist(i,j) = dist(h_i, h_j) = \min_{k,l=1..6} d(h_i^k, h_j^l)$, where h_i^k and h_j^l are the sides of the uncertainty hexagons h_i and h_j, and $d(a,b)$ is the Euclidean distance between two segments. The two segments i and j are considered as close to each other if:

$$0 < dist(i,j) \leqslant D_{int} \quad (2)$$

where D_{int} is the maximum internal width of a line (Fig. 3.a). It is computed from the width of the filter used by the edge detection (cf. Section 2). Any pair of segments verifying (1) and (2) is then considered as a possible line.

Let C_{ij} be such a pair. Let O'_i and E'_i (resp. O'_j and E'_j) the projections of O_i and E_i (resp. O_j and E_j) on the supporting line of j (resp. i) (Fig. 3.b). If the segments $[O'_i, E'_i]$ and j (resp. $[O'_j, E'_j]$ and i) has a common part T_i^j (resp. T_j^i), i and j are called *overlapping parallel* segments. C_{ij} is a line edge if the overlapping part is greater than the minimum length of a line, D_{min}. We considered D_{min} must be greater than D_{int}, in order to ensure line edge is longer than thick. Thus C_{ij} must verify:

$$\min(l_{T_i^j}, l_{T_j^i}) \geqslant D_{min} \quad (3)$$

where $l_{T_i^j}$ and $l_{T_j^i}$ are the lenghts of T_i^j and T_j^i.

A pair C_{ij} verifying (1), (2) and (3) is associated with three zones Z_{ext}, Z_{int} and Z'_{ext} which respectively represent the left external, internal and right external regions of the candidate line edge (Fig. 4.a). Z_{int} is the quadrilateral defined by T_i^j and T_j^i. Z_{ext} (resp. Z'_{ext}) is a rectangle defined by T_i^j (resp. T_j^i) and D_{ext}, which is the mean external width of a line and which is considered equal to six times the standard deviation of the smoothing filter. Let $\overline{Z_{ext}}$, $\overline{Z_{int}}$ and $\overline{Z'_{ext}}$ be the mean values of the pixels of the original image in the zones Z_{ext}, Z_{int} and Z'_{ext}. If the pair C_{ij} result from a line edge contour, $\overline{Z_{int}}$ is superior or inferior to the others. However, because of the noise and the discretization of the image signal, the mean value of the pixels in a given zone is all the less significative as this zone is small. From their definition and equation (3), the minimum surface of Z_{ext} and Z'_{ext} is $D_{ext} \times D_{min}$, which is experimentally large enough to $\overline{Z_{ext}}$ and $\overline{Z'_{ext}}$ be significative. However, from equations (1), (2) and (3), the surface of Z_{int} has no lower bound. Then we arbitrarily consider that $\overline{Z_{int}}$ is not significative if the surface of Z_{int} is less than a given constant D_{surf}, which is roughly $(D_{min})^2$ in our test data set. In this case, the profile of the line edge only includes Z_{ext} and Z'_{ext}: We consider that C_{ij} is a roof edge if the local maxima of the Gradient of the Gaussian which generated the segments i and j have opposite signs (Fig. 4.b). This simplified profile is not robust but allows the roof edge to be distinguished from the double step edge (Fig. 1.b).

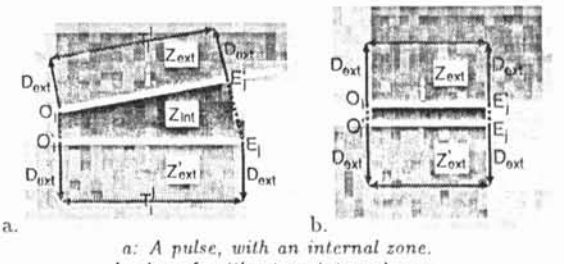

a: A pulse, with an internal zone.
b: A roof, without an internal zone.

Figure 4. The two sorts of line edge.

To sum up, a pair C_{ij} is generated by a line edge if it verifies (1), (2), (3) and:

$$\begin{cases} Sgn(GRAD(i)) \neq Sgn(GRAD(j)), \\ \qquad \text{with } Surface(Z_{int}) < D_{surf}, \\ \overline{Z_{int}} > \max(\overline{Z_{ext}}, \overline{Z'_{ext}}) \text{ or } \overline{Z_{int}} < \min(\overline{Z_{ext}}, \overline{Z'_{ext}}), \\ \qquad \text{with } Surface(Z_{int}) \geqslant D_{surf}. \end{cases} \quad (4)$$

If several pairs verify these equations for a same segment i, the segment j is selected so as to be the closest to i. The pair C_{ij} then become the line edge $C\{i\}\{j\}$, which is completely defined by its profile $F_{C\{i\}\{j\}}$ and its two chains Ch and Ch'. For the moment, each of these chains includes a single segment, i and j respectively. We now try and continue the chains using segments which do not yet belong to a line edge.

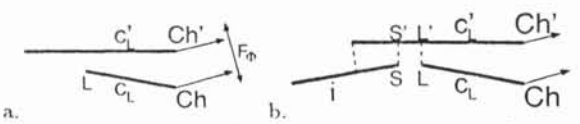

a: A free extremity L and its continued segment c'_L.
b: A continuing segment i.

Figure 5. The continued and continuing segment

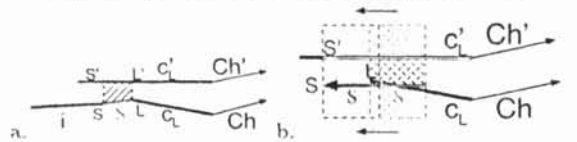

a: An undetected segment S. b: An artificial segment S.

Figure 6. Detection of the extremities.

4. CONTINUING A LINE EDGE

Let Φ be a line edge. It is defined by a profile F_Φ and two ordered chains of segments Ch and Ch'. A so-called *free extremity* of a line edge is the extremity of one of the chains which projects on the other chain. The segment on which this free extremity is projected is called *continued segment*. Let c_L be a segment from Ch having a free extremity L and c'_L be the continued segment of Ch' on which L projects (Fig. 5.a). A part of the segment c'_L is not yet used to form the line edge Φ. We then search for a segment i which do not yet belong to a line edge, such that $C_{ic'_L}$ verifies (1), (2), (3) and (4), i.e. such that i and c'_L form a line edge C. This line edge must have the same profile and the same orientation as Φ. The segment i is called the *continuing segment* of the line edge Φ at L.

Let S be the origin of i such that S is on the same side as L with respect to c'_L; i and c_L have the same orientation, given by the line edge Φ. Let S' and L' be the respective projections of S and L on c'_L. We can deduce from the study of the ordered set of points (S,L,L',S') that the line edges C and Φ form either the same line, either two different connected lines or two different non connected lines. In the optimal case, S and L are the same point: the segment i is connected to the chain Ch at L.

When the segment i intersects the line (L,L') in Y, we consider that there are a possible Y-shape junction between the two line edges Φ and C and also a third line edge. The line edge Φ is then continued using the segments [L,Y] and i.

When the segment i does not intersect the line (L,L') and C and Φ form the same line edge, (S,L,L',S') corresponds to a zone of the same kind as Z_{int}, in which the segment [S,L] has not been detected (Fig. 6.a). This anomaly is caused either by a line edge whose width is close to that of the filter used by the edge detection or by an unbalanced line edge which divides the original image into two regions having very different intensity levels. If there is only one line edge, we consider that the pair C_p including segments [S,L] and [S',L'] must satisfy equations (1), (2), (3) and (4). However, as the distance (S,L) may be arbitrarily long, equation (3) can not be verified and the surfaces of the external zones defined by C_p no longer have lower bounds. Therefore, the first condition of equation (4) is only true if either $Surface(Z_{ext}) \leqslant D_{surf}$ or $Surface(Z'_{ext}) \leqslant D_{surf}$. If C_p verify these restricted conditions, the line edge Φ is continued using the segments [L,S] and i.

This process is iterated until all the free extremities of Φ can not be continued. Such a method provides good results on the body of the line edge but the extremities of the line edge are not precisely located. The junctions between the extremities of a line edge and other edges often decreases the quality of the segments. In most cases, only one of the two segments constituting the extremities of the line edge is detected. This segment is the continued segment c'_L of the chain Ch', associated with the free extremity L of the chain Ch'. This case is similar to the continuation of a line edge, except that there is no continuing segment which allows the chain Ch to be continued at L. We thus create an artificial segment s such that it forms a line edge of minimum width with c'_L, s and c_L are parallel with a full overlapping and the middle of s is on c_L. s is then gradually moved towards the extremity of the line edge. When either equation (4) is no longer verified or the projection S' of the extremity S of s projects onto the extremity of c'_L, the extremity of the line edge is reached. The segment [S,L] is then added to the chain Ch and the point S' becomes the new extremity of c'_L: The line edge Φ is complete.

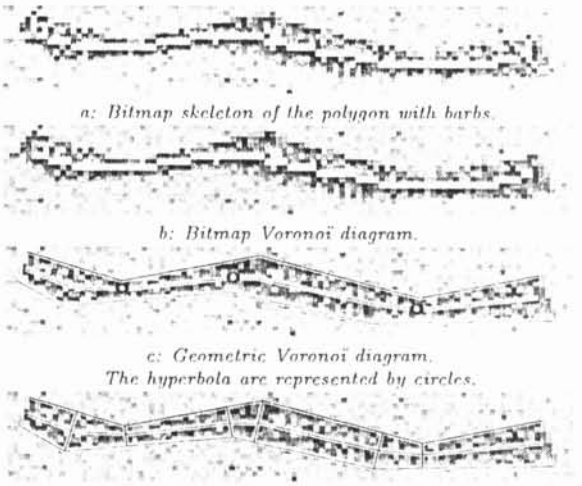

a: Bitmap skeleton of the polygon with barbs.
b: Bitmap Voronoï diagram.
c: Geometric Voronoï diagram. The hyperbola are represented by circles.
d: Our simple geometric method.

Figure 7. Computation of the peak.

All the line edges of the image are processed in that way. We now have to solve a last problem: the computation of the peaks.

5. COMPUTATION OF THE PEAKS

The ideal peak of a line edge is defined as the location of the physical discontinuity which generates the line. Unfortunately, this location is hard to obtain. As the mean width of a line edge never exceeds a few pixels, we consider that the peak is centred on the line. Respecting our conventions, the centre corresponds to the set of inner points equally distanced from the two chains of segments representing the line edge. We compared four methods to compute these points:

- A skeletonization [13] of the polygon obtained by connecting the extremities of the two chains of segments (Fig. 7.a): The result is a completely connected graph of pixels and is located at the exact centre of the line edge. However, the detected peaks are chains of pixels instead of segments. Moreover, the extremities of line edges, as well as the portions of line edges with a high curvature, are provided with parasitic barbs.
- A bitmap Voronoï diagram [11] in this same polygon: We consider that a pixel belongs to the digram if it is equally distanced from at least two non consecutive segments of the polygon and if there is no other segment which is closer to the pixel (Fig. 7.b). Although this method does not produce barbs, the resulting peaks are also chains of pixels and the extremities of the line edges are truncated.

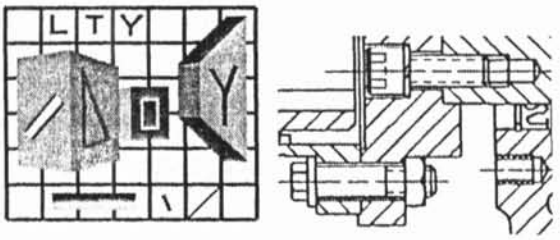

A synthesized noisy image and a technical drawing.

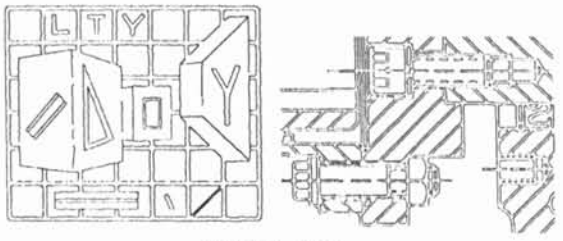

The step edges.

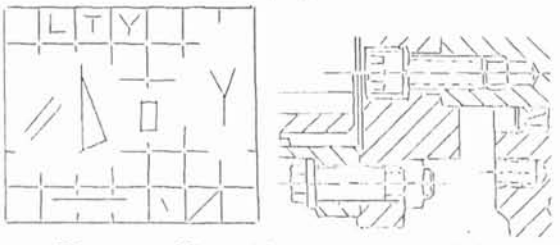

The extracted lines with our geometric method.

Figure 8. Two examples of our results.

- A geometric Voronoï diagram [1] in the polygon (Fig. 7.c): This method has a high complexity and produces piecewise defined curves, made of portions of straight lines and parabols, which cannot be easily used.
- A geometric method which gives an approximation of the centre of the two chains of segments (Fig. 7.d): All the extremities of the segments belonging to one of the chains are projected on the other. The projected points and the extremities of the segments create new segments. The chain determined by the middle points of these segments form the peak. As the two chains of segments representing the line edge are locally parallel, the new chain obtained in this way is close to a geometric Voronoï diagram but is easier to use.

6. EXPERIMENTAL RESULTS

Experiments have been performed on many kinds of numerical images. We present here only synthesized noisy image and technical drawing, in Figure 8.

If few lines edges are not detected, the most part of lines edges is globally relevant and very smoothed. The search for the extremities, as explained in section 4, continues the line edges whose ending segments are not detected in the original contour image. Line edges and staircases are efficiently identified by their profile. However, the polygonal approximation of curved line edges generates segments which are too small to be considered parallel with overlapping.

7. CONCLUSION

This paper describes a method to identify line contours, such that roof and pulse edges, from step edges. A line edge is modelled as overlapping parallel segments having the profile of a line edge. Thus, our line detector can deal with both steps and lines. We use a simple geometric algorithm to substitute every extracted line edge for a single line. Experimentations prove the reliability and robustness of our approach. Few line edges are actually missed and extracted lines are well located. Connectivity between other edges is globally reliable, and we are currently working on the location of all kinds of junctions between step and line edges.

ACKNOWLEDGMENTS

Many thanks to Gérald Masini and Sylvain Petitjean for proofreading draft copies of this paper and for their constructive comments, suggestions and incentives.

REFERENCES

[1] H. Amet. *Méthodes géométriques et algorithmiques pour la planification de trajectoires.* PhD thesis, Université Nancy I, van, dec 1990.

[2] J. Canny. A Computational Approach to Edge Detection. *IEEE Transactions on PAMI*, 8(6):679–698, 1986.

[3] R.T. Chin, H.K. Wan, D.L. Stover, and R.D. Iverson. A One-Pass Thinning Algorithm and Its Parallel Implementation. *Computer Vision, Graphics and Image Processing*, 40:30–40, 1987.

[4] R. Deriche. Fast Algorithms for Low-Level Vision. *IEEE Transactions on PAMI*, 12(1):78–87, 1990.

[5] G. Giraudon. Edge Detection from Local Negative Maximum of Second Derivative. In *Proceedings of IEEE Conference on Computer Vision and Pattern Recognition, San-Francisco, CA (USA)*, pages 643–645, 1985.

[6] G. Giraudon. An Efficient Edge Following Algorithm. In *Proceedings of 5th Scandinavian Conference on Image Analysis, Stockholm (Sweden)*, volume 2, pages 547–554, 1987.

[7] E. Hancock and J. Kittler. Relaxational Refinement of Intensity Ridges. In *Proceedings of 11th International Conference on Pattern Recognition, Den Haag (Netherlands)*, volume 3, pages 459–463, September 1992.

[8] J. Hasegawa, H. Kubota, and J. Toriwaki. Automated Construction of Image Processing Procedures by Sample-Figure Representation. In *Proceedings of 8th International Conference on Pattern Recognition, Paris (France)*, pages 586–588, 1986.

[9] J.-G. Leu and L. Chen. Polygonal Approximation of 2-D Shapes Through Boundary Merging. *Pattern Recognition Letters*, 7(4):231–238, 1988.

[10] D. Marr and E. Hildreth. Theory of Edge Detection. AI-Memo 518, MIT, 1980.

[11] F. Preparata and M.I. Shamos. *Computational Geometry, an Introduction.* Springer-Verlag, Berlin, 1985.

[12] E. Salari and P. Siy. The Ridge-Seeking Method for Obtaining the Skeleton of Digital Images. *IEEE Transactions on Systems, Man, and Cybernetics*, 14(3):524–528, 84.

[13] J. Serra. *Image Analysis and Mathematical Morphology.* Academic Press, London, 1982.

[14] G.E. Sotak, J.R. Boyer, and K.L. Boyer. Comments on "Fast Convolution with Laplacian-of-Gaussian Mask". *IEEE Transactions on PAMI*, 11(12):1329–1332, 1989.

[15] S. Tabbone. *Multi-scale junction and edge detection with subpixel accuracy.* PhD thesis (in french), february 1994.

[16] K. Wall and P. Danielsson. A Fast Sequential Method for Polygonal Approximation of Digitized Curves. *Computer Vision, Graphics and Image Processing*, 28:220–227, 1984.

[17] D. Ziou. Line Detection Using an Optimal IIR Filter. *Pattern Recognition*, 24(6):465–478, 1991.

[18] D. Ziou and R. Mohr. An Experience on Automatic Selection of the Edge Detectors. In *Proceedings of 11th International Conference on Pattern Recognition, Den Haag (Netherlands)*, volume 3, pages 586–589, 1992.